Energy Proceedings
Vol 33, 2023
ISSN 2004-2965

Study on factors affecting the sealing integrity of cement in CCUS well

Zhang Zhi [1*], Cai Nan [1], Liu Jinming [2], Zhao Yuanjin [1]

1 State Key Laboratory of Oil and Gas Reservoir Geology and Exploitation(Southwest Petroleum University), Chengdu, Sichuan 610500, China

2 Drilling and Production Engineering Research Institute of CNOOC EnerTech-Drilling & Production Co., 300457, Tianjin China

(*Corresponding Author: wisezh@126.com)

ABSTRACT

In the long-term storage process of CO_2 storage wells, the integrity of the cement is vulnerable to damage or even failure due to factors such as cementing quality, corrosion, stress change, etc., resulting in microcracks or leakage channel, resulting in the inability to guarantee the effectiveness of the storage. For this reason, this paper establishes a mechanical model of downhole casing-cement-formation combination in CCUS well, and studies the influence of wellbore pressure, temperature change, performance parameters of cement, etc. on the stress distribution of cement; The leakage characteristics of the combination are studied through the sealing integrity test of the combination, and the influence of different factors on the CO_2 leakage rate is discussed in combination with the leakage model of the cement. The research results show that (1) the integrity failure of the cement mainly reflects the failure of the seal due to the leakage channel, which can not achieve effective sealing; (2) The leakage rate of CO_2 is directly proportional to the permeability and cross-sectional area of the leakage channel, but the influence of the size of the cement on the leakage is limited; (3) The CO_2 leakage rate increases significantly with the increase of the pressure and temperature of the storage layer, and both of them are nonlinear. (4) The leakage rate of CO_2 is basically proportional to the crack width of cement. In theory, when the crack width of cement reaches 640 μm, the leakage rate of CO_2 exceeds the safety value, and the leakage rate of CO_2 increases exponentially with the increase of the crack opening of cement. The slight change of the crack opening will greatly increase the leakage rate of CO_2. This paper reveals the potential leakage path and law of cement in CCUS well, and the research results can provide guidance for the effectiveness of long-term storage design of CCUS well.

Keywords: CCUS well, sealing integrity of cement, casing- cement- formation combination, failure analysis of cement

NONMENCLATURE

Symbols	
A	*Circular cement cross-sectional area （m^2）*
a	*Inner radius of casing (mm)*
b	*Outer radius of casing/inner radius of cement (mm)*
c	*Outer radius of cement (mm)*
d	*Outer radius of formation (mm)*
E	Elastic modulus (MPa)
E_c	Elastic modulus of cement (MPa)
E_f	Elastic modulus of formation rock (MPa)
E_s	Elastic modulus of casing (MPa)
E_{st}	Young's modulus of steel (MPa)
h	Crack opening degree (mm)
k	Permeability (mD)

This is a paper for International CCUS Conference 2023 (ICCUSC2023), April 14-15, 2023, Beijing, China.

k_s	Permeability coefficient of cement seepage, k_s=1.07636×10^{-14} k
L_c	Length of cement column (m)
L_g	The length of the gas column at the top of the annulus (m)
L_m	Length of annular liquid column (m)
M	Average molecular weight of gas (*Kg/mol*)
p	Actual pressure(MPa)
p_c	Cement top pressure (MPa)
p_{c1}	External extrusion force of casing (MPa)
p_{c2}	Contact pressure of the second bonding surface of the cement (MPa)
p_i	Pressure inside the casing (MPa)
p_f	Formation pressure (MPa)
P_t	Pressure in the wellhead annulus (MPa)
p_{sc}	Standard pressure (MPa)
q_{sc}	Gas rate at the top of cement（m^3/d）
r	Cylinder radius (mm)
T	Actual temperature (K)
T_{sc}	Standard temperature (K)
T_{wh}	Temperature at the wellhead (K)
v	Poisson's ratio of materials (dimensionless)
v_c	Poisson's ratio of cement (dimensionless)
v_f	Poisson's ratio of strata and rocks (dimensionless)
v_s	Poisson's ratio of casing (dimensionless)
w	Crack width (mm)

z	Cement depth (m)
ε_ϑ	Tangential strain (dimensionless)
ε_z	Axial strain (dimensionless)
α	Material linear expansion coefficient (K^{-1})
α_c	Cement linear expansion coefficient (K^{-1})
α_f	Linear expansion coefficient of formation rock (K^{-1})
α_s	Expansion coefficient of casing line (K^{-1})
σ_r	Radial stress (MPa)
σ_ϑ	Tangential stress (MPa)
σ_z	Axial stress (MPa)
σ_{rs}	Radial stress of casing (MPa)
$\sigma_{\vartheta s}$	Radial stress of casing (MPa)
σ_{rc}	Radial stress of cement (MPa)
σ_{rf}	Formation radial stress (MPa)
$\sigma_{\vartheta c}$	Tangential stress of cement (MPa)
$\sigma_{\vartheta f}$	Formation tangential stress (MPa)
μ	CO_2 viscosity（mPa·s）
δ_{rci}	Radial deformation of cement inner wall (mm)
δ_{rco}	Radial deformation of cement outer wall (mm)
δ_{rso}	Outer diameter deformation of casing (mm)
δ_{rfi}	Radial deformation of the second bonding surface of the cement (mm)
δ_r	Radial deformation of cylinder (mm)
δR	Effective micro annular gap (μm)
ΔT	Temperature change value (℃)
ρ_m	Density of annular liquid in wellbore (g/cm^3)

1. INTRODUCTION

In recent years, global warming has caused a large number of extreme climate problems, such as the sustained drought in East Africa, which has led to over 20 million people facing food security issues. Pakistan's heavy rainfall triggered floods, resulting in over 1700 deaths and nearly 8 million people being displaced. The extremely hot and exceptionally dry weather in Europe has resulted in 15000 deaths. The continuous emission of CO_2 will inevitably exacerbate air pollution and the greenhouse effect, posing a serious challenge to the human living environment and posing a serious threat to human life, health and safety. Actively addressing climate change has become a global consensus and trend[1],[2].

CO_2 capture, storage, and utilization (CCUS) refers to the process of separating, capturing, and injecting

CO_2 from concentrated industrial or related energy sources into suitable formations deep underground, and storing it underground or utilizing it through physical and chemical processes. CCUS is considered an effective method to slow down the accumulation of greenhouse gases in the atmosphere and oceans, and one of its main challenges is the integrity of carbon sequestration wells[3]。The CO_2 concentration in the carbon storage well is relatively high. As time goes by, due to pressure changes and chemical corrosion, the cement in the injection well degrades, creating a leakage channel, which leads to CO_2 migration from the reservoir to a shallow aquifer or surface, affecting the integrity of the sealed wellbore and increasing the risk of wellbore leakage during the CO_2 storage period[4]. In 2019, Mohammadreza et al.[5] studied the degradation effect of CO_2 on cement properties. In 2021, Katherine et al.[6] compared the effects of CO_2 and H_2O on casing and cement corrosion under different conditions through experiments and explored the corrosion mechanism. The integrity and service risk assessment of the wellbore during long-term CO_2 storage are key challenges that need to be addressed urgently in CCUS wells. However, existing research focuses on the corrosion effect of CO_2 on cement, neglecting the study of leakage channels. Therefore, this article analyzes the mechanism of CO_2 corrosion damage to the cement and the corrosion penetration rate of CO_2 on the cement stone, establishes a mechanical model of the casing cement formation combination, analyzes the influence of downhole operation parameters on the mechanical integrity of the cement, and conducts sealing test experiments to analyze the leakage characteristics of the combination, and quantifies the pore and crack sizes of the cement. Finally, a leakage model of CO_2 along the main leakage path of the cement was established, and sensitivity analysis was conducted on key parameters (cement permeability, cement length, pressure difference, etc.) to evaluate the sealing ability of the cement in the well. Research can provide a basic theory for ensuring the integrity of CO_2 storage wells.

2. MECHANISM OF CO_2 CORROSION DAMAGE OF CEMENT

The corrosion of cement in CO_2 storage wells can be divided into three stages: the first stage is the dissolution of CO_2 in water. When CO_2 containing water diffuses into the cement matrix, CO_2 combines with water (wet supercritical CO_2 or CO_2 dissolved in water) to form H_2CO_3, as shown in equation (1). The second stage is the carbonization of cement, that is, free calcium hydroxide and hydrated calcium silicate (C-S-H) gel are gradually dissolved under the action of H_2CO_3 to generate calcium carbonate precipitation, as shown in Equations (2)~(5). The third stage is the dissolution of calcium carbonate. In the previous stage, the reaction product calcium carbonate is dissolved by excessive CO_2, and the reaction process is shown in equations (6) to (7) [7]. The above three stages of reactions result in the formation of obvious progressive alteration zones within the cement under CO_2 erosion, as shown in Fig. 2. [8].During the cement carbonization stage, the precipitation of $CaCO_3$ reduces the porosity of the cement, but excessive CO_2 leads to the dissolution of $CaCO_3$ during the leaching stage. In the end, the permeability and porosity of the cement stone increase, while the compressive strength decreases, manifested by the fracture and looseness of the cement stone, ultimately losing its protective effect on the wellbore, leading to CO_2 leakage to the surface [9].

$$CO_2 + H_2O \leftrightarrow H_2CO_3 \leftrightarrow H^+ + HCO_3^- \leftrightarrow 2H^+ + CO_3^{2-} \quad (1)$$

$$Ca(OH)_2(s) + 2H^+ + CO_3^{2-} \rightarrow CaCO_3(s) + 2H_2O \quad (2)$$

$$Ca(OH)_2(s) + H^+ + HCO_3^- \rightarrow CaCO_3(s) + 2H_2O \quad (3)$$

$$[C_{3,4}\text{-}S_2\text{-}H_8](s) + 2H^+ + CO_3^{2-} \rightarrow CaCO_3(s) + SiO_xOH_x(s) \quad (4)$$

$$[C_{3,4}\text{-}S_2\text{-}H_8](s) + H^+ + HCO_3^- \rightarrow CaCO_3(s) + SiO_xOH_x(s) \quad (5)$$

$$CO_2 + H_2O + CaCO_3(s) \leftrightarrow Ca^{2+} + 2HCO_3^- \quad (6)$$

$$CaCO_3(s) + 2H^+ \leftrightarrow CO_2 + Ca^{2+} + H_2O \quad (7)$$

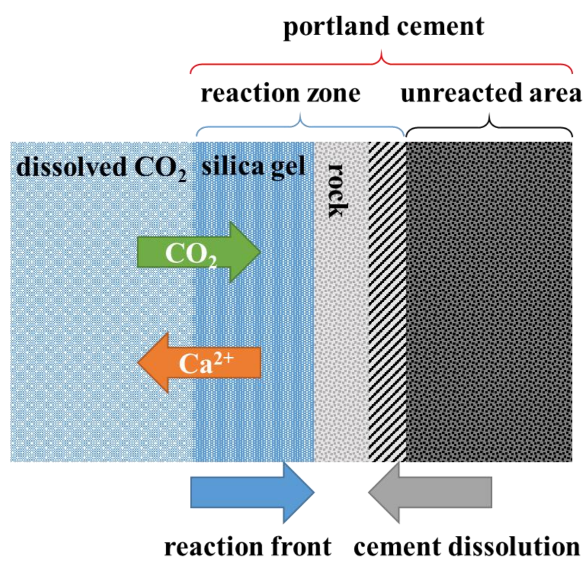

Fig. 1. Cement layer structure in contact with CO_2 rich fluids

3. MECHANICAL PROPERTY OF CASING- EMENT-FORMATION COMBINATION

3.1 Mechanical model

Assuming that the composite body is in a triaxial stress state, the deformation is axisymmetric, the interface bonding of the composite body is uniform, and the initial stress value of the cement is 0. Using a plane strain model for mechanical analysis of the entire composite body, establish a mechanical model for the cement [10]. Considering the temperature effect, the tangential strain is:

$$\varepsilon_\theta = \frac{1}{E}\left[\sigma_\theta - \nu\left(\sigma_z - \sigma_r\right)\right] + \alpha \Delta T \tag{8}$$

The axial strain is:

$$\varepsilon_z = \frac{1}{E}\left[\sigma_z - \nu\left(\sigma_\theta + \sigma_r\right)\right] + \alpha \Delta T \tag{9}$$

Without considering axial strain, then $\varepsilon_z \approx 0$, as can be obtained from the above equation:

$$\sigma_z = \nu\left(\sigma_\theta + \sigma_r\right) - \alpha E \Delta T \tag{10}$$

Bringing equation (10) into equation (8) yields:

$$\varepsilon_\theta = \frac{1}{E}\left[(1-\nu^2)\sigma_\theta - (\nu^2+\nu)\sigma_r + (1-\nu)\alpha E \Delta T\right] \tag{11}$$

The radial deformation of the cylinder is obtained as:

$$\delta_r = \frac{r}{E}\left[(1-\nu^2)\sigma_\theta - (\nu^2+\nu)\sigma_r + (1-\nu)\alpha E \Delta T\right] \tag{12}$$

According to the Lame formula, the radial stress distribution of the casing can be obtained:

$$\sigma_{rs} = \frac{p_i a^2 - p_{c1} b^2}{b^2 - a^2} - \frac{\left(p_i - p_{c1}\right) a^2 b^2}{b^2 - a^2} \frac{1}{r} \tag{13}$$

The tangential stress distribution of the casing is:

$$\sigma_{\theta s} = \frac{p_i a^2 - p_{c1} b^2}{b^2 - a^2} + \frac{\left(p_i - p_{c1}\right) a^2 b^2}{b^2 - a^2} \frac{1}{r^2} \tag{14}$$

The radial deformation of the outer wall of the casing can be obtained as:

$$\delta_{rso} = \frac{b}{E_s}\left(1-\nu_s^2\right)\left[\frac{2a^2 p_i - p_{c1}(a^2+b^2)}{b^2-a^2}\right] + \frac{b}{E_s}\left(\nu_s + \nu_s^2\right) p_{c1} + b(1-\nu_s)\alpha_s \Delta T \tag{15}$$

For the cement, the contact pressures on the inner and outer walls are p_{c1} and p_{c2}, respectively. The radial stress in the cement is:

$$\sigma_{rc} = \frac{p_{c1} b^2 - p_{c2} c^2}{c^2 - b^2} - \frac{\left(p_{c1} - p_{c2}\right) b^2 c^2}{c^2 - b^2} \frac{1}{r^2} \tag{16}$$

The tangential stress of the cement is:

$$\sigma_{\theta c} = \frac{p_{c1} b^2 - p_{c2} c^2}{c^2 - b^2} + \frac{\left(p_{c1} - p_{c2}\right) b^2 c^2}{c^2 - b^2} \frac{1}{r^2} \tag{17}$$

The radial deformation of the inner diameter of the cement is:

$$\delta_{rci} = \frac{b}{E_c}\left(1-\nu_c^2\right)\left[\frac{p_{c1}(b^2+c^2) - 2c^2 p_{c2}}{c^2-b^2}\right] + \frac{b}{E_c}\left(\nu_c + \nu_c^2\right) p_{c1} + b(1-\nu_c)\alpha_c \Delta T \tag{18}$$

The radial deformation of the second bonding surface of the cement is:

$$\delta_{rco} = \frac{c}{E_c}\left(1-\nu_c^2\right)\left[\frac{2b^2 p_{c1} - p_{c2}\left(b^2+c^2\right)}{c^2-b^2}\right] + \frac{c}{E_c}\left(\nu_c + \nu_c^2\right) p_{c2} + c\left(1-\nu_c\right)\alpha_c E_c \Delta T \tag{19}$$

The radial and tangential stresses in the formation rocks are:

$$\sigma_{rf} = \frac{p_{c2} c^2 - p_f d^2}{d^2 - c^2} - \frac{\left(p_{c2} - p_f\right) b^2 c^2}{d^2 - c^2} \frac{1}{r^2} \tag{20}$$

$$\sigma_{\theta f} = \frac{p_{c2} c^2 - p_f d^2}{d^2 - c^2} + \frac{\left(p_{c2} - p_f\right) c^2 d^2}{d^2 - c^2} \frac{1}{r^2} \tag{21}$$

The radial deformation at the second bonding surface of the cement is:

$$\delta_{rfi} = \frac{c}{E_f}\left(1-\nu_f^2\right)\left[\frac{p_{c2}\left(c^2+d^2\right) - 2d^2 p_f}{d^2-c^2}\right] + \frac{c}{E_f}\left(\nu_f + \nu_f^2\right) p_{c2} + c\left(1-\nu_f\right)\alpha_f \Delta T \tag{22}$$

Due to the constant radial deformation at the second bonding surface of the cement, equation (19)=equation (22) can be solved as follows:

$$U p_{c1} + V p_{c2} + W p_f = E_c E_f \Delta T\left[\left(1-\nu_f\right)\alpha_f - \left(1-\nu_c\right)\alpha_c\right] \tag{23}$$

Werein：

$$U = \frac{2b^2}{c^2 - b^2} E_f\left(1-\nu_c^2\right) \tag{24}$$

$$W = \frac{2b^2}{d^2 - c^2} E_c\left(1-\nu_f^2\right) \tag{25}$$

$$V = \frac{2c^2\nu_c^2 + \left(c^2-b^2\right)\nu_c - \left(c^2+b^2\right)}{c^2-b^2} E_f - \frac{\left(d^2+c^2\right) - 2c^2\nu_f^2 + \left(d^2-c^2\right)\nu_f}{d^2-c^2} E_o \tag{26}$$

3.2 Analysis of Factors Influencing the Mechanical Properties of Cement

Example basic parameter values: outer diameter of casing 177.8mm, wall thickness 9.17mm, cement thickness range of 25mm, Poisson's ratio of casing 0.3, elastic modulus of casing 206GPa, Poisson's ratio of cement 0.03-0.23, elastic modulus of cement 7-15GPa, Poisson's ratio of formation 0.18, and elastic modulus of formation 4GPa.

3.2.1 The influence of effective internal pressure

The distribution of radial and circumferential stresses at different radii and lengths of the mud ring under different internal pressures is shown in Fig. 2. The internal stresses are taken as 10MPa, 20MPa, 30MPa, 40MPa, and 50MPa, respectively. From Fig. 2. (a), it can be seen that the radial stress of the cement gradually decreases from the first interface to the second interface, but the magnitude of the decrease is slowing down. With the continuous increase of internal stress, the radial stress of different radius lengths of the cement gradually increases, and the maximum radial stress appears at the first interface of the cement. Fig. 2. (b) shows the distribution of circumferential stress in cement with different radius lengths. It can be seen that the circumferential stress in cement increases with the increase of internal pressure, and the amplitude of the increase is relatively uniform with the change of wellbore diameter.

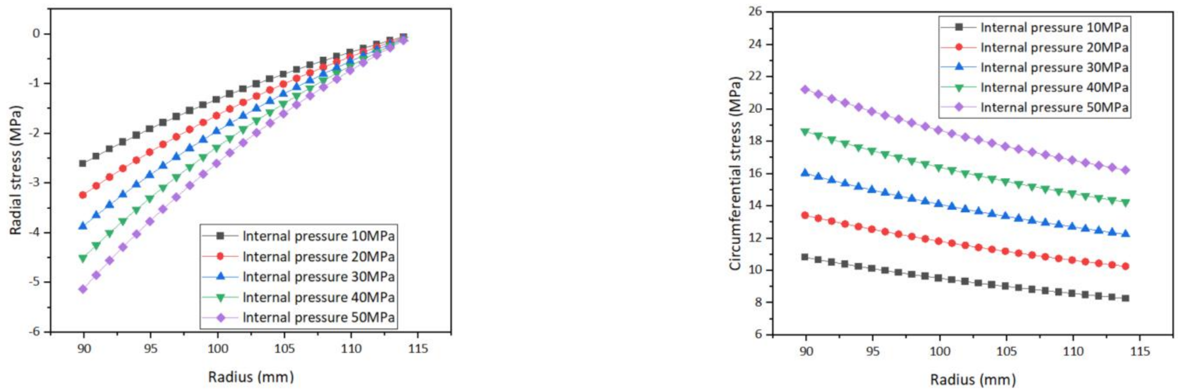

(a) The distribution of radial stress (b) The distribution of circumferential stress

Fig. 2. Radial and circumferential stress distribution of mud ring under different internal pressures with different radius lengths

3.2.2 The influence of temperature variation

The distribution of radial and circumferential stresses at different radius lengths of the cement during wellbore temperature changes is calculated as shown in Fig. 3. The temperature changes are taken as 20 ℃, 40 ℃, 60 ℃, 80 ℃, 100 ℃, and 120 ℃, respectively. From Fig. 3. (a), it can be seen that with the continuous increase of temperature change, the radial stress of any radius length of the cement gradually increases, but the amplitude of increase from the first interface to the second interface of cementing gradually decreases. Overall, the positive change in temperature did not result in a significant increase in radial stress. Fig. 3. (b) shows the distribution of circumferential stress at different radius lengths of the cement. It can be seen that the circumferential stress at any radius length of the cement gradually increases with increasing temperature.

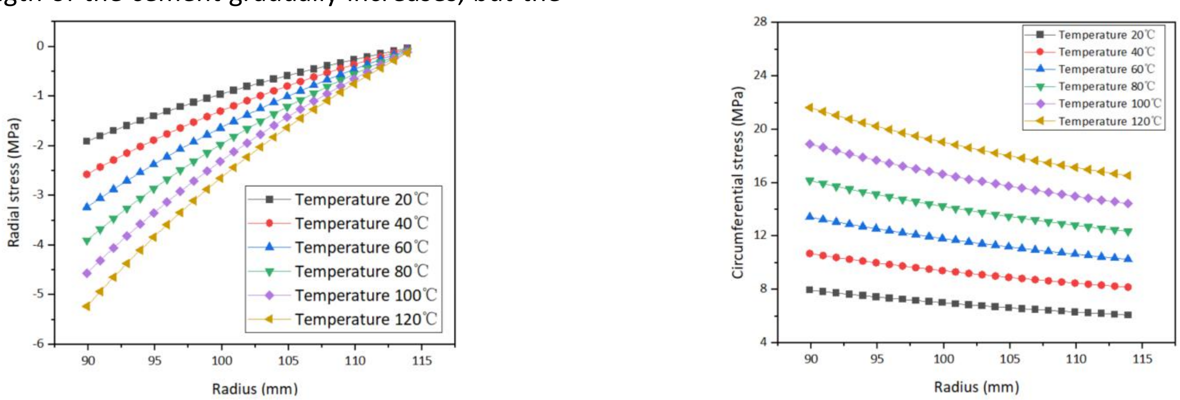

(a) The distribution of radial stress (b) The distribution of circumferential stress

Fig. 3. Radial and circumferential stress distribution of cement with different radius lengths under different wellbore temperature changes

3.2.3 The influence of elastic modulus of cement

The distribution of radial stress and circumferential stress at different radius lengths under different elastic moduli of cement is shown in Fig. 4. The elastic moduli of cement are taken as 7GPa, 9GPa, 11GPa, 13GPa, and 15GPa, respectively. From Fig. 4. (a), it can be seen that with the continuous increase of the elastic modulus of the cement, the radial stress at any radius length of the cement gradually increases, and the amplitude of the increase from the first interface to the second interface gradually decreases. Fig. 4. (b) shows the circumferential stress distribution of cement with different radius lengths. It can be seen that the circumferential stress of any radius length of cement gradually increases with the increase of elastic modulus of cement.

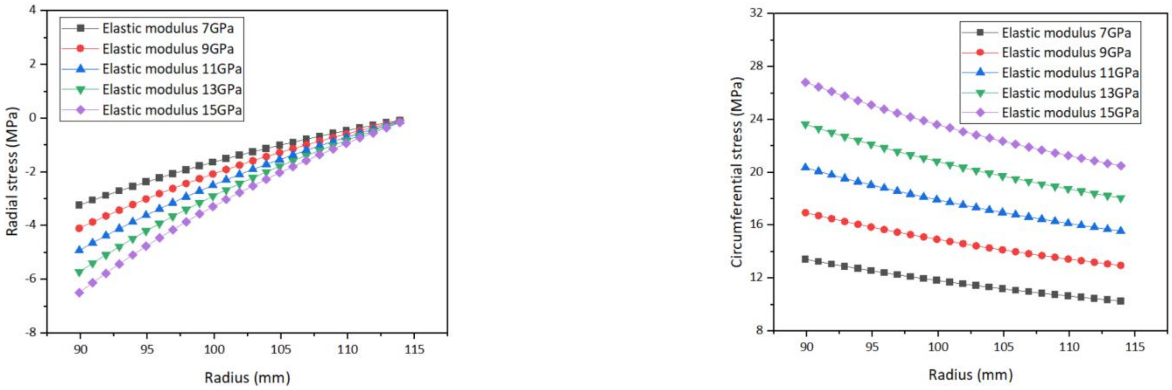

(a) The distribution of radial stress (b) The distribution of circumferential stress

Fig. 4. Radial and circumferential stress distribution of cement with different radius lengths under different elastic modulus

3.2.4 The influence of Poisson's ratio of cement

The distribution of radial stress and circumferential stress for different radius lengths under different cement Poisson's ratios is shown in Fig. 5. The cement Poisson's ratios are 0.03, 0.08, 0.13, 0.18, and 0.23, respectively. From Fig. 5. (a), it can be seen that as the Poisson's ratio of the cement increases, the radial stress gradually decreases, but the magnitude of the decrease is not significant. The closer the Poisson's ratio is to the second interface of the cementing, the smaller the impact. Fig. 5. (b) shows the distribution of circumferential stress at different radius lengths of the cement. It can be seen that the circumferential stress at any radius length of the cement gradually decreases with an increase in the Poisson's ratio of the cement.

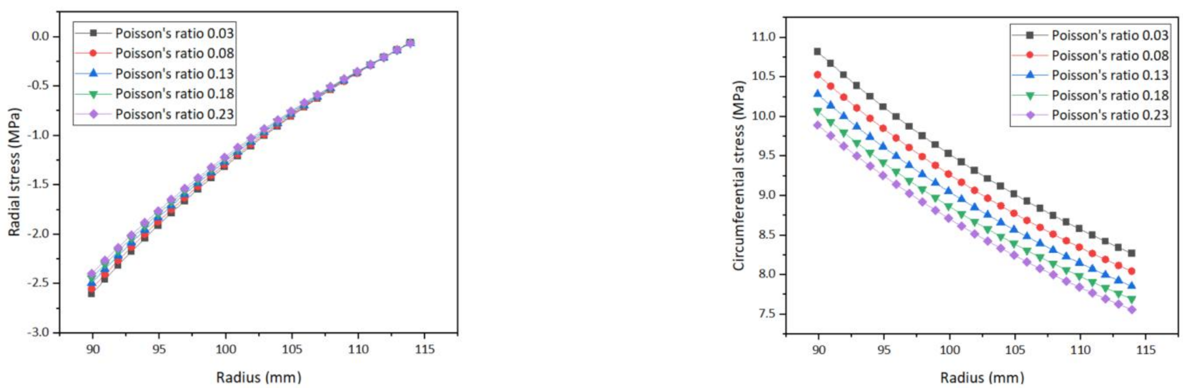

(a) The distribution of radial stress (b) The distribution of circumferential stress

Fig. 5. Radial and circumferential stress distribution of cement with different radius lengths under different Poisson's ratio

4. CO_2 LEAKAGE MODEL ALONG CEMENT

4.1 The main leakage path of CO_2 along the cement

The main leakage pathways related to CO_2 and cement can be divided into two categories. Firstly, through the cement itself, the permeability of cement may increase due to potential changes in the porous structure of the cement and the formation of cracks inside the cement; The second is through the micro annular gap between the cement and the casing or between the cement and the formation, as shown in Figure 6. Therefore, studying the leakage of CO_2 along different paths and conducting quantitative analysis is crucial for evaluating the integrity of the cement. The upward migration of CO_2 along the leakage path is a process typically controlled by the formation pressure gradient and CO_2 gravity, influenced by changes in CO_2 properties such as density, viscosity, enthalpy, and phase state along the path, and accompanied by heat transfer between the escaping CO_2 and the leakage path, as well as heat conduction in the formation.

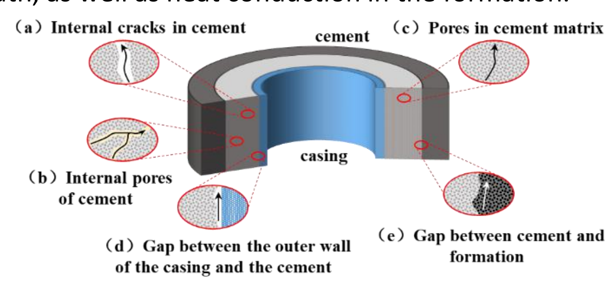

Fig. 6. CO_2 leakage pathway through cement

4.2 The leakage model of CO_2 along the cement

Improper design of cement slurry and/or lack of adhesion between cement and casing or formation can lead to gas infiltration into the annulus, and Darcy's law can be effectively used to simulate such gas flow. According to Darcy's law, the following expressions for pressure gradient and fluid velocity are obtained[11]:

$$\frac{dp}{dz}=\frac{\mu v}{k_s}=\frac{\mu q}{Ak_s} \quad (27)$$

In equation (27), k_s is the permeability coefficient of cement seepage, and the conversion coefficient to permeability k is 1.07636×10^{-14}, i.e. $k_s=1.07636\times10^{-14}k$. When flowing into the cement column, the gas flow rate will vary with the depth of cement z. To illustrate this change, the gas state equation is introduced:

$$pV=ZnRT \quad (28)$$

Substitute the standard pressure p_{sc}, standard temperature T_{sc}, actual pressure p, and temperature T to obtain:

$$p=\frac{P_{sc}ZT}{T_{sc}} \quad (29)$$

Calculate the gas rate q_{sc} at the top of the cement using equation (27) as follows:

$$q_{sc}=\frac{kAT_{sc}}{\mu ZTp_{sc}}p\frac{dp}{dz} \quad (30)$$

When flowing into the cement column, the changes in gas temperature, viscosity, and Z-coefficient are likely to be minimal, and can be represented by the average values T_i, L_i, and Z_i evaluated under initial conditions. Under these assumptions, the following relationship between gas rate q_{sc}, formation pressure p_f, and cement top pressure p_c is derived based on formula (30) [12]:

$$q_{sc}=\frac{kAT_{sc}}{2L_c\mu_i Z_i T_i p_{sc}}(p_f^2-p_c^2) \quad (31)$$

Converted to oilfield standard units, equation (31) is written as:

$$q_{sc}=\frac{0.011174kAT_{sc}}{L_c\mu_i Z_i Tp_{sc}}(p_f^2-p_c^2) \quad (32)$$

Considering the time effect, the pressure on the top of cement within n unit time lengths can be expressed as:

$$P_c^n=P_t^{n-1}+0.0098\rho_m L_{\mathrm{m}}^{n-1}+0.0098\frac{P_t^{n-1}M}{ZR'T_{wh}}L_{\mathrm{g}}^{n-1} \quad (33)$$

The leakage rate through cement is a function of cement permeability, cement quality, and barrier pressure difference. Estimate the pressure difference based on the bottom hole pressure below the barrier and the hydrostatic pressure gradient at the top of the barrier. As CO_2 begins to leak from the lower part of the well and migrate along the wellbore, it begins to expand and the pressure difference on the barrier further increases, leading to more CO_2 migrating into the wellbore [13]。

Assuming that CO_2 stored in the reservoir can leak through a complex path and then accumulate in the gas chamber of the annulus before escaping to the surface, the calculation of CO_2 leakage through the cement matrix can be written as follows using Darcy's law:

$$q_{\mathrm{cement}}=\frac{11.174T_{sc}}{ZP_{sc}T}\left(\frac{kA}{\mu L}\right)(p_f^2-(p_c^n)^2) \quad (34)$$

Due to the fact that the effective flow rate through open cracks/cracks is a cubic function of aperture length [14]. Therefore, the following formula (35) can be used to calculate the leakage flow rate in cement cracks. The crack opening does not take into account the irregularity of the crack surface, groove, and transverse continuity, and the simplified crack opening is considered in the equation.

$$q_{\mathrm{crack}}=\frac{9.3116\times10^{-4}T_{sc}}{ZP_{sc}T}\left(\frac{wh^3}{\mu L}\right)(p_f^2-(p_c^n)^2) \quad (35)$$

When a casing with radius R_c and wall thickness h_c is placed under internal pressure P, its radius will expand:

$$\delta R_c=\frac{R_c^2P}{E_{st}h_c} \quad (36)$$

The cement in the casing annulus with a thickness of R_{cem} will shrink:

$$\delta R_{cem,A}=\frac{\Delta R_{cem}P}{E_{cem}} \quad (37)$$

The radius of the cement cylinder in a pipeline with a radius of R_T will shrink with increasing pressure:

$$\delta R_{cem,T}=\frac{R_TP_T}{E_{cem}} \quad (38)$$

Effective micro ring gap δR can be determined by the following formula:

$$Q=\frac{\pi R_c\Delta P}{6\mu L}\delta R^3 \quad (39)$$

The formula for calculating the micro annular leakage rate between the cement casing interface and the cement formation interface is shown in equation (40).

$$q_{\mathrm{micro\text{-}annulus}}=\frac{1.86\times10^{-3}T_{sc}}{ZP_{sc}T}\left(\frac{\pi D_c\delta R^3}{\mu L}\right)(p_f^2-(p_c^n)^2) \quad (40)$$

4.3 Case study

Select the parameter range shown in Table 1 to simulate and study the effects of cement permeability, crack size, and micro annulus on the migration of CO_2 leakage from underground to surface. Research has shown that the permeability of correctly solidified G-grade cement is about 0.001mD. Unless the cement has been degraded or not properly solidified, significant flow will not occur. The permeability of inferior cement is about 0.010mD, and the permeability of defective cement is about 0.100mD. The range of permeability set for degraded cement is shown in the table below.

Table 1 Basic parameters for calculating CO_2 leakage rate

Parameter	Unit	Value				
Standard pressure	Pa	0.1×10^6				
Standard temperature	K	273.15				
Well depth	m	3500				
Casing diameter	mm	177.8				
Cement thickness	mm	25	50	75	100	125
Cement permeability	mD	0.01	0.5	1	5	10
Crack opening degree	μm	0.3	1	9	20	35
Crack width	μm	1	10	100	600	1000
Micro annulus	μm	1	3	9	15	30

To make geological storage feasible, it is safe and feasible to assume a leakage rate of less than 1% of stored CO_2 every 100 years. CO_2 leakage may occur through one or more of the three mechanisms: cement matrix, cement cracks, and cement microenvironment. This article is for simplification of calculations and does not consider the cross effects of various mechanisms, only for separate consideration. Assuming the annual target storage capacity of a certain block is 300000 tons, considering the supercritical CO_2 state density of 800kg/m^3, and the annual leakage rate not exceeding 100m^3, it is safe. Below is an analysis of the leakage rate under different parameter conditions for each path.

4.3.1 Leakage along the pores of the cement matrix

The permeability values are 0.01mD, 0.05mD, 1mD, 5mD, and 10mD, respectively, covering the permeability of normal sealing of G-grade cement and the permeability of different degrees of degradation. As shown in the figure 7, when there are no other defects in the cement, the leakage rate of CO_2 is basically proportional to the permeability of the cement. When the permeability is 0, the leakage rate of CO_2 is also 0. In theory, when the permeability reaches around 3.2mD, the annual leakage exceeds 100m^3. In actual working conditions, the degradation permeability of cement stone is much lower than this value.

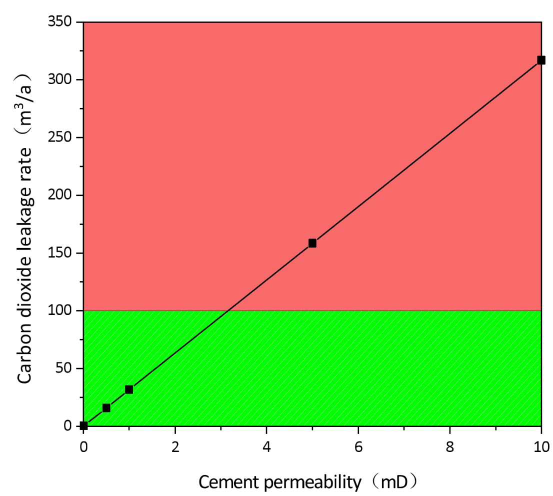

Fig. 7. Leakage rate of CO_2 along the matrix under different cement permeability

4.3.2 Leakage along cement cracks

The calculation results of CO_2 leakage rate along the cement matrix under different crack width conditions are shown in Fig. 8. Maintain a crack opening of 1 μm. The crack width values are 1 respectively μm, 10 μm, 100 μm, 600 μm and 1000μm. The value is based on the crack size measured experimentally. As shown in the figure, when there are no other defects in the cement, leakage only occurs in the vertical direction. The leakage rate of CO_2 is basically proportional to the crack width of the cement. When the crack width is 0, the CO_2 leakage rate is also 0. In theory, when the crack width of cement reaches 640 µ At around m, the leakage rate of CO_2 exceeds 100m^3/a.

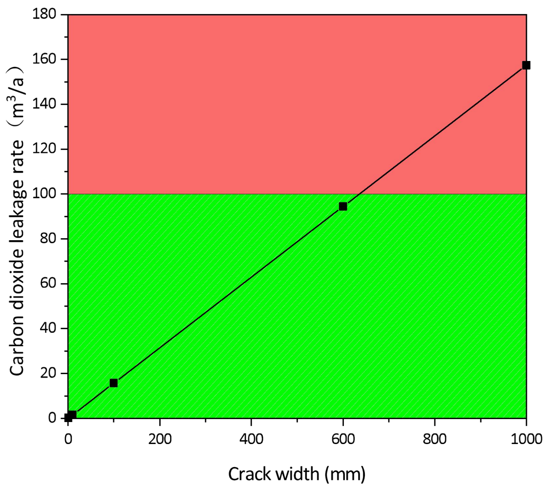

Fig. 8. Leakage rate of CO_2 along the matrix under different crack width

Fig. 9. shows the calculation results of CO_2 leakage rate along the cement matrix under different crack opening conditions. Maintain crack width of 1 µm. The crack opening values are 0.3 µm, 1 µm, 9 µm, 20 µm and 35 µm respectively. From the figure, it can be seen that when there are no other defects in the cement, leakage only occurs in the vertical direction. The leakage rate of CO_2 increases exponentially with the increase of the crack opening of the cement, and any small change in the crack opening will significantly increase the CO_2 leakage rate. In theory, when the opening degree of cement cracks reaches 8.8 µm At around m, the leakage rate of CO_2 exceeds 100m^3/a.

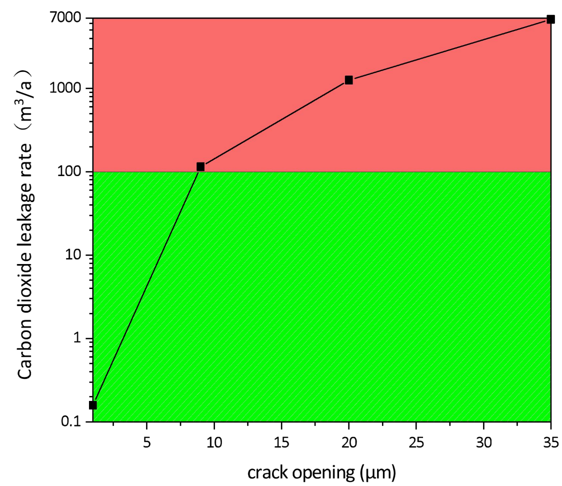

Fig. 9. CO_2 leakage rate along cracks under different cement crack opening conditions

4.3.3 Leakage along cement cracks

Fig. 10. shows the calculation results of CO_2 leakage rate along the interface micro ring gap under different cement micro ring size conditions. The size values of the micro ring are 1 µm, 3 µm, 6 µm, 9 µm and 15 µm。From the figure, it can be seen that when there are no other defects in the cement, leakage only occurs in the vertical direction. The leakage rate of CO_2 increases exponentially with the increase of the size of the cement microenvironment, and any small change in crack opening will significantly increase the CO_2 leakage rate. In theory, when the opening degree of cement cracks reaches 2.1 µ At around m, the leakage rate of CO_2 exceeds 100m^3/a.

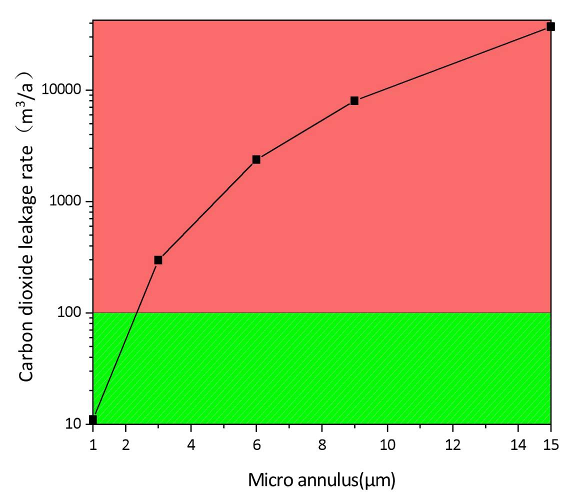

Fig. 10. Leakage rate of CO_2 along the micro ring gap under different cement micro annulus sizes

4.3.4 The impact of leakage channel cross-sectional area

Other conditions are fixed, assuming five different leakage channel cross-sectional areas, namely 0.016 m^2, 0.036 m^2, 0.06 m^2, 0.09 m^2, and 0.12 m^2, corresponding to a cement thickness range of 25mm~125mm. The influence of cement leakage channel cross-sectional area on the annual CO_2 leakage is discussed, as shown in Fig. 11. From the figure, it can be seen that the CO_2 leakage rate is directly proportional to the cross-sectional area of the leakage channel. The larger the cross-sectional area, the greater the leakage amount. However, due to the limitation of the thickness of the cement, the change in cross-sectional area has limited impact on the CO_2 leakage rate. If the cross-sectional area of the leakage channel is 0, there is no leakage.

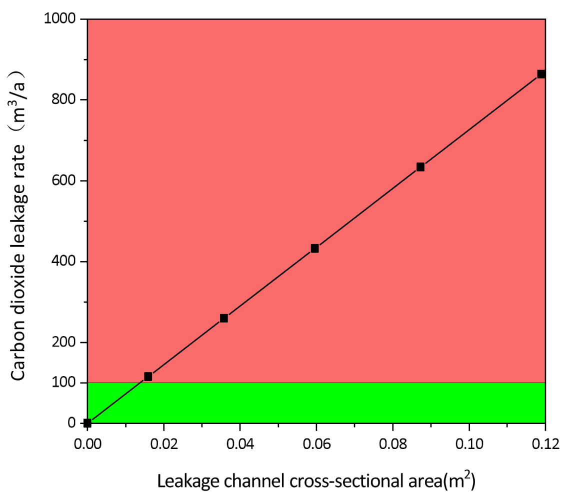

Fig. 11. Impact of the cross-sectional area of the vertical leakage channel on the CO_2 leakage rate

5. CONCLUSIONS

(1) the integrity failure of the cement mainly reflects the failure of the seal due to the leakage channel, which can not achieve effective sealing.

(2) The leakage rate of CO_2 is directly proportional to the permeability and cross-sectional area of the leakage channel, but the influence of the size of the cement on the leakage is limited.

(3) The CO_2 leakage rate increases significantly with the increase of the pressure and temperature of the storage layer, and both of them are nonlinear.

(4) The leakage rate of CO_2 is basically proportional to the crack width of cement. In theory, when the crack width of cement reaches 640 μm, the leakage rate of CO_2 exceeds the safety value, and the leakage rate of CO_2 increases exponentially with the increase of the crack opening of cement. The slight change of the crack opening will greatly increase the leakage rate of CO_2.

ACKNOWLEDGEMENT

The authors are grateful for the support of the National Natural Science Foundation of China (U22A20164), the National Natural Science Foundation of China (52074234), the Innovative Research Team of Sichuan Province (2020JDTD0016), and the Technology Cooperation Project of China Petroleum-Southwest Petroleum University Innovation Consortium (2020CX040100).

DECLARATION OF INTEREST STATEMENT

The authors declare that they have no known competing financial interests or personal relationships that could have appeared to influence the work reported in this paper. All authors read and approved the final manuscript.

REFERENCE

[1] Zou Caicai, Xiong Bo, Xue Huaqing, et al. The role of new energy in carbon neutral. Petroleum Exploration and Development 2021; 48(2):480–491.

[2] Hu Yongle, Hao Mingqiang, Chen Guoli, et al. CO_2 displacement and burial technology and practice in China. Petroleum Exploration and Development 2019;46(4): 753–766.

[3] MILLAR R J, FUGLESTVEDT J S, FRIEDLINGSTEIN P, et al. Emission budgets and pathways Consistent with limiting warming to 1.5 ℃ . Nature Geoscience 2017;10:741–747.

[4]Meyer V, Houdu E, Poupard O, et al. Quantitative risk evaluation related to long term CO_2 gas leakage along wells. Energy Procedia 2009;1(1):3595–3602.

[5] Bagheri M, Shariatipour S M, Ganjian E. A Study on the Chemo-Mechanical Alteration of Cement in CO_2 Storage Sites. Paper presented at the SPE Europec featured at 81st EAGE Conference and Exhibition. 2019.

[6] Katherine Beltrán Jiménez, Anwar I, Gebremariam K F, et al. Assessment of corrosion in the Interface Casing - Cement and its Effect on the Leakage Potential. Paper presented at the SPE/IADC International Drilling Conference and Exhibition. 2021.

[7] Si Nan, Zhang Liwei, Gan Manguang, et al. Geological storage environment CO_2 Experimental study on the influence of pressure on the degree of cement carbonization. Chinese Journal of Electrical Engineering 2022;42(09):3126–3135.

[8] Arlèt-Gouédard V., Rimmelé G., Porcherie O., et al. A solution against well cement degradation under CO_2 geological storage environment. International Journal of Greenhouse Gas Control 2009: 206–216.
[9] Duguid A, Radonjic M, Scherer G W. Degradation of cement at the reservoir/cement interface from exposure to carbonated brine. International Journal of Greenhouse Gas Control 2011;5(6):1413–1428.
[10] Chu Wei, Shen Jiyun, Yang Yunfei, et al. Calculation of Micro Annular Gap in the Combination of Casing Cement and Surrounding Rock under Continuously Varying Internal Pressure. Petroleum Exploration and Development 2015;42(03):379–385.
[11] Rocha-Valadez T, Hasan A R, Mannan S, et al. Assessing Wellbore Integrity in Sustained-Casing-Pressure Annulus. Spe Drilling & Completion 2014;29(01):131–138.
[12] Aas, B., Sørbø, J., Stokka, S. et al. Cement Placement with Tubing Left in Hole during Plug and Abandonment Operations. Paper presented at the IADC/SPE Drilling Conference and Exhibition. 2016.
[13] Patil P A, Chidambaram P, Amir M , et al. FEP Based Model Development for Assessing Well Integrity Risk Related to CO_2 Storage in Central Luconia Gas Fields in Sarawak. Paper presented at the International Petroleum Technology Conference. 2021.
[14] Snow D T. Rock Fracture Spacings, Openings, and Porosities Closure. Journal of the Soil Mechanics & Foundations Division 1968;94(1):73–92.